

This is a very elegant result obtained from our perturbation theory. It says that the transition probability of an atom from one level to another under the influence of a random perturbation is the Fourier transform of the autocorrelation function of the perturbation divided by \hbar^2 . Many processes in atomic frequency standards are caused by random perturbations. These include, for example, relaxation caused by the random motion of an atom in an inhomogeneous magnetic field. Fourier components at the frequency ω_0 may be strong enough to create transitions among energy levels. Equation (1.2.128) above is just an evaluation of the intensity of these Fourier components. The problem treated earlier of an incident flux $I(v)$ of photons on an atom is of the same nature and can be treated in a similar manner. We will come back to this point in Chapter 4.

We should note, however, that we have calculated the effect of the random perturbation on the product $c_k c_k^*$ which is the probability of finding the atom in state k . We could not treat easily here the case in which terms such as $c_n c_k^*$ are present. Such products create interference terms in the integral and it is best to treat them with the help of the density matrix formalism which we now introduce.

1.3 ENSEMBLE OF ATOMS: THE DENSITY MATRIX

The previous sections dealt with the behaviour of a single atom or spin in various environments. In practice, however, and especially in atomic frequency standards one deals with large quantities of atoms in interaction with each other and with their environment. In this case the previous analysis is not sufficient and phenomena such as relaxation and coherence in ensembles of atoms, an important concept in the subject treated in this monograph, cannot be introduced directly in the analysis made up to now. However, the density matrix formalism, which we shall use throughout, deals with these concepts in a very natural manner and, furthermore, introduces equations to handle them. We do not plan to give a complete treatise on the subject here, since several texts and monographs exist in this field (Fano 1957, Vanier 1971). We would like, however, to recall the general ideas which make the density matrix formalism necessary. We would like also to give the general properties of the density operator ρ with sufficient background to make the reading of the following chapters relatively easy.

1.3.1 The Density Operator

A single atom is characterised by a wavefunction ψ which can be expressed in terms of basis eigenvectors $|u_n\rangle$ by means of the relation

$$|\psi\rangle = \sum_n c_n |\psi_n\rangle = \sum_n c_n e^{-(i/\hbar)E_n t} |u_n\rangle = \sum_n a_n |u_n\rangle \quad (1.3.1)$$

where c_n and a_n depend on time. The outcome of a measurement of the state of the atom would give $|a_n|^2$ as the probability of finding the atom in state $|u_n\rangle$. This is a basic consequence of the quantum mechanical behaviour of the atomic world. If one of the a_n is equal to one, say $a_2 = 1$, the atom is then to be found with certainty in state 2. If the space consists of only two states, 1 and 2, for example, and if $a_1 = a_2 = 1/\sqrt{2}$, then, the probability of finding the particle in either state is $1/2$. That is, the outcome of a measurement of the state of the atom or system would give the system a 50 % chance to be found in either state. This is what we can call a quantum mechanical probability.

However, if we deal with two atoms, then, the atom denoted by 1 may be described by the wavefunction $\psi(1)$ which may be different from the wavefunction $\psi(2)$ describing the atom denoted by 2. In the case of a larger number of atoms it is natural to think that the atoms are distributed in the various states in a statistical manner. This new effect is caused by the fact that we are dealing with a large quantity of atoms. Furthermore, we do not have all information on the state of the various atoms and this forces us into a statistical approach. We must thus associate with the measurements of the properties of one of the atoms a new probability which we call p_k and which essentially gives the number of atoms in state ψ_k . To illustrate let us say that we want to measure the average value \bar{M} of the magnetisation of an ensemble of atoms distributed in a statistical manner among the various states ψ_k . Then, for an atom in one of the states, the expectation value of the magnetic moment operator μ_{op} is given in quantum mechanics as

$$\langle \mu \rangle = \langle \psi_k | \mu_{\text{op}} | \psi_k \rangle. \quad (1.3.2)$$

If N_k atoms out of the total number, N , are in state ψ_k , then the statistical average value of $\langle \mu \rangle$ is $\overline{\langle \mu \rangle}$ given by

$$\overline{\langle \mu \rangle} = \frac{1}{N} \sum_k N_k \langle \psi_k | \mu_{\text{op}} | \psi_k \rangle \quad (1.3.3)$$

$$\overline{\langle \mu \rangle} = \sum_k p_k \langle \psi_k | \mu_{\text{op}} | \psi_k \rangle \quad (1.3.4)$$

where

$$p_k = N_k / N. \quad (1.3.5)$$

If all the atoms were characterised by the same wavefunction ψ_n we would have $p_n = 1$ and $\overline{\langle \mu \rangle} = \langle \mu \rangle$. This is called a pure state in the statistical sense. In such a case we have all the information about the ensemble. The quantum mechanical expectation value is essentially a

statistical average value for a pure state. In general, however, this is not the case. The state ψ_k can then be written

$$|\psi_k\rangle = \sum_n a_{kn} |u_n\rangle \quad (1.3.6)$$

which, when replaced in equation (1.3.4) gives

$$\langle\mu\rangle = \sum_n \sum_m \left(\sum_k p_k a_{kn}^* a_{km} \right) \langle u_n | \mu_{op} | u_m \rangle. \quad (1.3.7)$$

The term $\sum_k p_k a_{kn}^* a_{km}$ is then defined as the matrix element of an operator ρ called the density operator:

$$\rho_{mn} = \sum_k p_k a_{kn}^* a_{km} = \overline{a_n^* a_m} \quad (1.3.8)$$

where the bar on $\overline{a_n^* a_m}$ means a statistical average. The order of the indices is chosen according to the general convention in this field (Tolman 1938). From the expression above we may then write

$$\overline{\langle\mu\rangle} = \text{Tr } \rho \mu. \quad (1.3.9)$$

$\text{Tr } \rho \mu$ means: add all the diagonal elements of the matrix obtained by making the product of the density matrix ρ by the matrix of the operator μ . This may be written for any macroscopic quantity, Q , belonging to a system and expressed in terms of an operator in quantum mechanics:

$$\overline{\langle Q \rangle} = \text{Tr } \rho Q. \quad (1.3.10)$$

Now, p_k is the probability that the system is in state ψ_k and a_{kn} is the projection of the vector $|\psi_k\rangle$ on the component $|u_n\rangle$. Then, if $m = n$ in equation (1.3.8) which defines ρ , we have

$$\rho_{nn} = \sum_k p_k a_{kn}^* a_{kn} \quad (1.3.11)$$

as the probability that the system is in state ψ_k and has vector component $|u_n\rangle$. This amounts to the probability that the system is in the eigenstate u_n . Or, in other words, ρ_{nn} gives the probability of finding the system in eigenstate u_n , and if N is the total number of systems in the ensemble, then $(\rho_{nn}N)$ is just the population of eigenstate u_n or level n . If $\rho_{nn} = 1$, which implies that $a_n = 1$ and that $p_k = 1$, it is a particular case in which all the systems are found with certainty in state $|\psi_k\rangle = |u_n\rangle$. All the information on the system is known and this is a pure state. This is a case often encountered in atomic beams which have been prepared by state selection, for example.

On the other hand, if $n \neq m$, we then have the cross product of the two amplitudes a_{kn} and a_{km} , associated with the two eigenvectors $|u_n\rangle$ and $|u_m\rangle$ respectively. If we write the state vector as

$$|\psi_k\rangle = \sum_n c_{kn}(0) \exp[-(i/\hbar)E_n t] |u_n\rangle \quad (1.3.12)$$

where $c_{kn}(0)$ is the initial value of $c_{kn}(t)$, then, we have

$$\rho_{nm} = \sum_k p_k c_{km}^*(0) c_{kn}(0) \exp[-(i/\hbar)(E_n - E_m)t] \quad (1.3.13)$$

$$\rho_{nm} = \rho_{nm}(0) \exp(-i\omega_{nm}t). \quad (1.3.14)$$

Since the time dependence has been removed from the $c_{kn}(0)$, then $\rho_{nm}(0)$ has no implicit time dependence and it is seen that the off-diagonal elements, if they do not equal zero, must oscillate with time at the angular frequency

$$\omega_{nm} = (E_n - E_m)/\hbar. \quad (1.3.15)$$

In a statistical ensemble, in thermal equilibrium, the phases of the c_{kn} are random and the off-diagonal elements are zero. We shall see below in an example, how off-diagonal elements can be created. ρ being an operator we may write

$$\rho|u_m\rangle = \sum_n \rho_{nm} |u_n\rangle. \quad (1.3.16)$$

If we multiply on the left by $\langle u_n|$, we obtain

$$\rho_{nm} = \langle u_n | \rho | u_m \rangle. \quad (1.3.17)$$

This is a simple relation that brings out the fact that the matrix ρ is expressed in the basis $\{|u_n\rangle\}$.

1.3.2 Properties of ρ

We give now several properties of ρ without rigorous proof. However, such proofs can be found in several texts listed in the bibliography.

(1) ρ is a Hermitian operator:

$$\rho_{nm} = \rho_{mn}^*. \quad (1.3.18)$$

(2) Since the diagonal elements represent the fractional population of the levels, we must have

$$\sum_n \rho_{nn} = \text{Tr } \rho = 1 \quad (1.3.19)$$

at all times, under all circumstances.

(3) Time dependence of ρ . The dependence of ρ on time can be obtained directly from Schrödinger's equation; we have

$$i\hbar \frac{d}{dt} |\psi\rangle = \mathcal{H}|\psi\rangle. \quad (1.3.20)$$

We replace $|\psi\rangle$ given by equation (1.3.1) in this equation and we obtain

obtain

$$\frac{da_k}{dt} = (i\hbar)^{-1} \sum_n a_n \langle k | \mathcal{H} | n \rangle \quad (1.3.21a)$$

$$\frac{da_k^*}{dt} = - (i\hbar)^{-1} \sum_n a_n^* [\langle k | \mathcal{H} | n \rangle]^*. \quad (1.3.21b)$$

Furthermore, we have

$$\frac{d}{dt} a_m^* a_n = a_m^* \frac{da_n}{dt} + \frac{da_m^*}{dt} a_n. \quad (1.3.22)$$

Replacing equations (1.3.21a,b) in this last equation and averaging over the ensemble, we obtain

$$\frac{d}{dt} \rho_{nm} = (i\hbar)^{-1} \sum_i (\mathcal{H}_{ni} \rho_{im} - \rho_{ni} \mathcal{H}_{im}) \quad (1.3.23)$$

which we write in a symbolic form as

$$\frac{d\rho}{dt} = (i\hbar)^{-1} [\mathcal{H}, \rho]. \quad (1.3.24)$$

The term in brackets is the commutator of \mathcal{H} and ρ and means the summation in equation (1.3.23). This equation is known as the analogue of Liouville's equation in classical statistical mechanics. It is basic in the formalism. It gives rise to the rate equations used in the solution of practical problems.

In the case that \mathcal{H} is independent of time, we have

$$\sum_i \mathcal{H}_{ni} = E_n$$

$$\sum_i \mathcal{H}_{im} = E_m$$

then

$$\frac{d\rho_{nm}}{dt} = (i\hbar)^{-1} \rho_{nm} (E_n - E_m)$$

and

$$\rho_{nm}(t) = \rho_{nm}(0) \exp(-i\omega_{nm} t). \quad (1.3.25)$$

This again says that the off-diagonal elements, created at time $t = 0$, oscillate with time at the angular frequency ω_{nm} . This result agrees with equation (1.3.14) derived previously. On the other hand if $n = m$, then

$$\rho_{nn}(t) = \rho_{nn}(0) = \text{Const.}$$

and the diagonal elements are independent of time when no perturbation is applied.

(4) The pure state. If all the information on the system is known with certainty, we do not require a statistical law to characterise its state and

we say that the system is in a pure state. We have encountered such a case earlier. A pure state is a very special case which requires a preparation of the ensemble like, for example, state selection. For a pure state the following relation holds:

$$\rho^2 = \rho \quad (1.3.26)$$

$$\text{Tr } \rho^2 = 1. \quad (1.3.27)$$

A typical case would be an ensemble with all systems in an eigenstate $|u_n\rangle$. Then, one of the diagonal elements of ρ is one and obviously we satisfy the above relations.

(5) The interaction representation. It is possible to express ρ in a representation that simplifies the notation, especially in the writing of rate equations. Equation (1.3.24) can be written as

$$\frac{d\rho}{dt} = (i\hbar)^{-1} (\mathcal{H}\rho - \rho\mathcal{H}). \quad (1.3.28)$$

If \mathcal{H} is independent of time the solution of this last equation is

$$\rho(t) = \exp[-(i/\hbar)\mathcal{H}_0 t] \rho(0) \exp[(i/\hbar)\mathcal{H}_0 t]. \quad (1.3.29)$$

Now, suppose that \mathcal{H} is of the form

$$\mathcal{H} = \mathcal{H}_0 + \mathcal{H}_1(t)$$

where \mathcal{H}_0 is time independent and $\mathcal{H}_1(t)$ is time dependent. We may then try a solution to equation (1.3.28) of the form

$$\rho(t) = \exp[-(i/\hbar)\mathcal{H}_0 t] \rho'(t) \exp[(i/\hbar)\mathcal{H}_0 t] \quad (1.3.30)$$

where $\rho'(t)$ contains a variation with time caused only by \mathcal{H}_1 . A straightforward calculation then gives

$$\frac{d}{dt} \rho'(t) = (i\hbar)^{-1} [\mathcal{H}_1(t), \rho'(t)] \quad (1.3.31)$$

where

$$\rho'(t) = \{\exp[(i/\hbar)\mathcal{H}_0 t]\} \rho(t) \{\exp[-(i/\hbar)\mathcal{H}_0 t]\} \quad (1.3.32)$$

and

$$\mathcal{H}_1(t) = \{\exp[(i/\hbar)\mathcal{H}_0 t]\} \mathcal{H}_1(t) \{\exp[-(i/\hbar)\mathcal{H}_0 t]\}. \quad (1.3.33)$$

Equation (1.3.31) describes the evolution of ρ in a representation that we call the interaction representation. The effect of \mathcal{H}_0 and $\mathcal{H}_1(t)$ have been separated. In the case $\mathcal{H}_1(t) = 0$ it is readily verified that $\rho'(t)$ is a constant of motion, $\rho'(0)$. In this type of case equation (1.3.30) becomes

$$\rho_{nm}(t) = \rho'_{nm}(0) \exp[(-i/\hbar)(E_n - E_m)t]. \quad (1.3.34)$$

In the case of angular momentum operators it is a simple matter to

show that the interaction representation amounts to expressing the evolution of variables in a system of axes which rotates at the Larmor frequency (Vanier 1971, p 35).

1.3.3 An example: an Ensemble of Spins, $S = \frac{1}{2}$, without Relaxation

In order to prepare ourselves for more complex situations in the analysis of the operation of atomic frequency standards, let us illustrate the previous concepts with an example borrowed from magnetic resonance. Let us assume that we have an ensemble of spins with magnetic moments $\mu_s = \gamma s \hbar S = -g_s \mu_B S$ in a magnetic field induction B_0 along the z axis. We are thus, as before, in the presence of systems which have two states with energy:

$$E_1 = \frac{1}{2}g_s \mu_B B_0 \quad (1.3.35)$$

$$E_2 = -\frac{1}{2}g_s \mu_B B_0. \quad (1.3.36)$$

We also assume that the spins are exposed to an oscillating field, in the x direction, with induction

$$\mathbf{B} = iB_x = iB_1 \cos \omega t. \quad (1.3.37)$$

We have already considered this problem for a single atom or spin in §1.2.3. We have found that the interaction Hamiltonian is (see equation (1.2.35))

$$\mathcal{H}_{12} = \frac{1}{4}g_s \mu_B B_1 [\exp(i\omega t) + \exp(-i\omega t)]. \quad (1.3.38)$$

From an earlier analysis we know that one of the exponential terms gives rise to a non-resonant term which is negligible compared with the resonant term created by the other exponential. We thus neglect one of the exponentials and use the rotating-wave approximation. Equation (1.3.23) can then be written for the individual elements of the density matrix. We obtain

$$d\rho_{11}/dt = \omega_1 \operatorname{Im}[\rho_{21}\exp(-i\omega t)] \quad (1.3.39)$$

$$d\rho_{22}/dt = -\omega_1 \operatorname{Im}[\rho_{21}\exp(-i\omega t)] \quad (1.3.40)$$

$$d\rho_{21}/dt = i\omega_0 \rho_{21} - i(\omega_1/2)(\rho_{11} - \rho_{22})\exp(i\omega t) \quad (1.3.41)$$

where $\omega_0 = (E_1 - E_2)/\hbar$. The equation for ρ_{12} is not required since we have $\rho_{21} = \rho_{12}^*$. This is the set of equations describing the evolution of a system of the ensemble. It is assumed that all the spins or systems obey this set of equations. The evolution of this ‘average’ spin is best seen in a particular case when the applied frequency ω is equal to the resonant frequency ω_0 . In that case, assuming that $\rho_{11} = 1$ and $\rho_{22} = \rho_{12} = 0$ at time $t = 0$, the solution is

$$\rho(t) = \begin{pmatrix} \frac{1}{2}(1 + \cos \omega_1 t) & \frac{1}{2}i \sin \omega_1 t \exp(-i\omega_0 t) \\ -\frac{1}{2}i \sin \omega_1 t \exp(i\omega_0 t) & \frac{1}{2}(1 - \cos \omega_1 t) \end{pmatrix}. \quad (1.3.42)$$

From this result it is observed that the resonant perturbation creates off-diagonal elements oscillating with time at the resonant frequency ω_0 . Their amplitude is modulated at the angular frequency

$$\omega_1 = \frac{g_s \mu_B}{\hbar} \frac{B_1}{2}.$$

The fractional population difference $\rho_{11} - \rho_{22}$ also oscillates with time at the frequency ω_1 . This result is essentially the same as that obtained earlier in §1.2.3 for a single spin. In the present case we have assumed $\rho_{11} = 1$, a pure state. It is thus not surprising that we obtain an identical result. This example, however, shows how the formalism can be applied.

The concept of $\frac{1}{2}\pi$ and π pulses is clearly made explicit in the present context. It is seen that if $\omega_1 t = \frac{1}{2}\pi$ we have

$$\rho_{11} = \rho_{22} = \frac{1}{2} \quad (1.3.43)$$

$$\rho_{12} = \frac{1}{2}i \exp(-i\omega_0 t). \quad (1.3.44)$$

Immediately after the pulse, the probabilities of occupation of the two levels are the same and the off-diagonal elements are maximum, oscillating at the resonant frequency ω_0 .

In terms of magnetic resonance concepts we can explain the above results in the following manner. Let us calculate the average magnetisation $\langle \mathbf{M} \rangle$ of an ensemble composed of N spins. We have

$$\langle M_i \rangle = \operatorname{Tr}(M_i \rho) \quad i = x, y, z \quad (1.3.45)$$

where the operator M_i is given by the relation

$$M_i = -N g_s \mu_B S_i \quad (1.3.46)$$

$$M_i = N \gamma_s \hbar S_i. \quad (1.3.47)$$

The operators S_i for a spin $\frac{1}{2}$ are given by the matrices of table 1.1.1. We then have

$$\langle M_x \rangle = -\frac{1}{2}N g_s \mu_B (\rho_{12} + \rho_{21}) \quad (1.3.48a)$$

$$\langle M_y \rangle = -\frac{1}{2}N g_s \mu_B i(\rho_{12} - \rho_{21}) \quad (1.3.48b)$$

$$\langle M_z \rangle = -\frac{1}{2}N g_s \mu_B (\rho_{11} - \rho_{22}). \quad (1.3.48c)$$

If we replace the matrix elements by their values we obtain

$$\langle M_x \rangle = -\frac{1}{2}N g_s \mu_B \sin \omega_1 t \sin \omega_0 t \quad (1.3.49a)$$

$$\langle M_y \rangle = \frac{1}{2}N g_s \mu_B \sin \omega_1 t \cos \omega_0 t \quad (1.3.49b)$$

$$\langle M_z \rangle = -\frac{1}{2}N g_s \mu_B \cos \omega_1 t. \quad (1.3.49c)$$

These results can be interpreted as follows. At time $t = 0$ all the individual spin vectors are distributed on a cone giving a net component of magnetisation $\langle M_z \rangle$. These spins are all in state 1. Upon the

application of the resonant radiation the component $\langle M_z \rangle$ is tipped towards the xy plane, meaning in a sense that the whole cone is tipped towards the xy plane. When $\omega_0 t = \frac{1}{2}\pi$, $\langle M_z \rangle = 0$ and $\langle M_x \rangle$, as well as $\langle M_y \rangle$, has a maximum value. The magnetisation oscillates in the xy plane at the resonant frequency ω_0 .

These concepts play a very important role in atomic frequency standards although, in general, in these devices we do not have a constant magnetisation present. In masers, for example, it is standard practice to extract information on the spins by means of $\frac{1}{2}\pi$ pulses. In caesium beam frequency standards the region of interaction between the atoms and the RF field is divided into two parts. As far as the density matrix is concerned, each interaction region acts as RF pulses.

1.3.4 Density Matrix with Relaxation Effects

In the previous example it was assumed implicitly that the spins were perturbed only by the electromagnetic field present. In many types of atomic frequency standards, the atoms are perturbed by various random interactions which give rise to relaxation. We have already introduced such a concept. In fact we have calculated in §1.2.9 a transition probability or rate from one level j to a level k due to the presence of a random perturbation. The result was

$$P_{jk} = \frac{1}{\hbar^2} \int_{-\infty}^{+\infty} G_{jk}(\tau) e^{-i\omega_0\tau} d\tau \quad (1.3.50)$$

where $G_{jk}(\tau)$ is the autocorrelation function of the random perturbation defined as

$$G_{kj}(\tau) = \langle k | \mathcal{H}_1(t - \tau) | j \rangle \langle j | \mathcal{H}_1(t) | k \rangle. \quad (1.3.51)$$

The starting point of the calculation was equation (1.2.121) which dealt only with the change of population of the level k . Thus, it applied only to the diagonal elements of the density matrix. It is standard procedure to include relaxation in the density matrix time-dependent equation as follows:

$$d\rho_{jj}/dt = (i\hbar)^{-1}[\mathcal{H}, \rho]_{jj} + \sum_k (\rho_{kk} P_{kj} - \rho_{jj} P_{jk}). \quad (1.3.52)$$

The first term in the equation includes the static interaction \mathcal{H}_0 and a time-dependent interaction $\mathcal{H}_1(t)$ which may represent the effect of an applied RF field. The second term represents the effect of relaxation increasing the population of level j at the expense of all other levels k . The third term represents relaxation decreasing the population of level j , atoms being distributed among levels k . In general, the P_{jk} are not equal. Furthermore the population of the levels tends to an equilibrium. In thermal equilibrium, without an electromagnetic field applied, no

radiation is emitted or absorbed and we have $[\mathcal{H}_1, \rho]_{jj} = 0$ and $d\rho_{jj}/dt = 0$. It follows that

$$\rho_{kk}^e P_{kj} = \rho_{jj}^e P_{jk} \quad (1.3.53)$$

where ρ_{jj}^e is the thermal equilibrium value of ρ_{jj} . We define a relaxation rate as

$$\gamma_{jk} = P_{jk}/\rho_{kk}^e \quad (1.3.54)$$

which, when replaced in equation (1.3.52), gives

$$d\rho_{jj}/dt = (i\hbar)^{-1}[\mathcal{H}, \rho]_{jj} + \sum_k (\rho_{kk} \rho_{jj}^e \gamma_{kj} - \rho_{jj} \rho_{kk}^e \gamma_{jk}). \quad (1.3.55)$$

When we need to consider only two levels, which is often the case in atomic frequency standards, we have

$$\gamma_{kj} = \gamma_{jk} = \gamma_1 \quad (1.3.56)$$

and, since

$$\sum_k \rho_{kk} = \sum_k \rho_{kk}^e = 1 \quad (1.3.57)$$

we then obtain:

$$d\rho_{jj}/dt = (i\hbar)^{-1}[\mathcal{H}, \rho]_{jj} + \gamma_1 (\rho_{jj}^e - \rho_{jj}). \quad (1.3.58)$$

The parameter γ_1 is called the population relaxation rate. In the absence of other perturbations such as electromagnetic radiation, ρ_{jj} , if perturbed from its equilibrium value, ρ_{jj}^e , at time $t = 0$, will return to equilibrium at a rate γ_1 or a time constant $T_1 = 1/\gamma_1$ according to the law

$$\rho_{jj} - \rho_{jj}^e = (\rho_{jj}(0) - \rho_{jj}^e) \exp(-t/T_1) \quad (1.3.59)$$

where $\rho_{jj}(0)$ is the value of $\rho_{jj}(t)$ at time $t = 0$, created by a means not specified in the present context. The value of ρ_{jj}^e at thermal equilibrium is given by the Boltzmann factor

$$\rho_{jj}^e = \exp[(-E_j/kT)] \left(\sum_m \exp[(-E_m/kT)] \right)^{-1}. \quad (1.3.60)$$

In frequency standards the spacing between the levels is very small compared with kT . Expanding in series and neglecting all terms in E_m/kT we obtain $\rho_{jj}^e = 1/m$. The levels, at equilibrium, are thus, in that case, all equally populated and equation (1.3.58) becomes

$$d\rho_{jj}/dt = (i\hbar)^{-1}[\mathcal{H}, \rho]_{jj} - \gamma_1 \left(\rho_{jj} - \frac{1}{m} \right) \quad (1.3.61)$$

where m is the number of levels in the manifold considered. In such a

case we necessarily have

$$\gamma_1 = mP_{km}. \quad (1.3.62)$$

This approach takes care only of the diagonal elements of the density matrix. However, it is possible to obtain a general analytical expression which makes explicit the effect of random perturbations on the off-diagonal elements of the density matrix. The theory in which this is developed is called the 'Bloch-Wangness-Redfield' approach. In Appendix 1C we give a summary of that theory. The general results are as follows.

For the diagonal elements, the resulting equation is identical to equation (1.3.58) above.

The off-diagonal elements relax towards a thermal equilibrium value equal to zero, as it should. The relaxation takes place at a rate which can be calculated from the autocorrelation function of the perturbation. In general, this rate is complex. Its imaginary part introduces a small frequency shift in the transition. We thus have

$$d\rho_{ij}/dt = (i\hbar)^{-1}[\mathcal{H}, \rho]_{ij} - (\gamma_2 + i\Delta\omega)\rho_{ij} \quad (1.3.63)$$

where γ_2 is a relaxation rate and $\Delta\omega$ is a frequency shift caused by the random perturbation. This can also be written as

$$d\rho_{ij}/dt = -i(\omega_{ij} + \Delta\omega)\rho_{ij} + (i\hbar)^{-1}[\mathcal{H}_1, \rho]_{ij} - \gamma_2\rho_{ij}. \quad (1.3.64)$$

The parameter γ_2 is called the coherence relaxation rate. Equation (1.3.64) above says that when no electromagnetic radiation is applied ρ_{ij} decreases with time at the rate γ_2 , or with the time constant $T_2 = 1/\gamma_2$, from a value $\rho_{ij}(0)$ which could have existed at time $t = 0$; thus

$$|\rho_{ij}(t)| = |\rho_{ij}(0)| \exp(-t/T_2). \quad (1.3.65)$$

In thermal equilibrium all off-diagonal elements are zero.

In general $\gamma_1 \neq \gamma_2$, because they are usually caused by different processes. Examples of relaxation processes we will have to consider in this monograph are: collisions between atoms and a foreign gas, collisions between atoms and the wall of a container, spin-exchange collisions, motion of atoms in inhomogeneous fields, direct escape from the ensemble and several others.

It should be pointed out that the additivity of coherent and incoherent perturbations, as is made explicit in equation (1.3.64), appears as a natural consequence of Redfield's theory as developed in Appendix 1C.

1.3.5 Example: an Ensemble of Spins with Relaxation

In this section we illustrate the effect of relaxation on an actual ensemble. To do this we use an ensemble of spin- $\frac{1}{2}$ particles that we have examined earlier to which we add relaxation as shown in figure 1.3.1. The rate equations for the density matrix elements are thus

$$d\rho_{11}/dt = \omega_1 \operatorname{Im}(\rho_{21} e^{-i\omega t}) - \gamma_1(\rho_{11} - \rho_{11}^e) \quad (1.3.66)$$

$$d\rho_{22}/dt = -\omega_1 \operatorname{Im}(\rho_{21} e^{-i\omega t}) - \gamma_1(\rho_{22} - \rho_{22}^e) \quad (1.3.67)$$

$$d\rho_{21}/dt = -i\omega_{21}\rho_{21} - \frac{1}{2}i\omega_1(\rho_{11} - \rho_{22})e^{i\omega t} - (\gamma_2 + i\Delta\omega)\rho_{21}. \quad (1.3.68)$$

Very similar expressions will be obtained in the analysis of the operation of atomic frequency standards. The only differences may be in the actual values of ρ_{21} and in the fact that we shall have to add in these expressions terms creating an equilibrium population different from ρ_{ii}^e . For the moment we give the procedure involved in solving these equations in two cases.

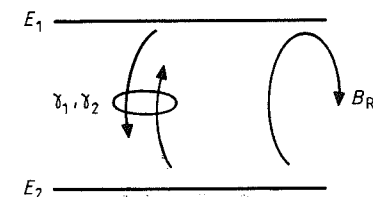


Figure 1.3.1 Illustration of the effect of a RF field and of relaxation on spins distributed between two energy levels E_1 and E_2 .

(A) Steady-state solution

In the case of equilibrium between the effect of relaxation and the applied electromagnetic field we have

$$\frac{d}{dt}(\rho_{11} - \rho_{22}) = 0. \quad (1.3.69)$$

Furthermore, we let the off-diagonal element oscillate at the angular frequency ω of the applied field

$$\rho_{21} = \rho_{12}^* = \frac{1}{2}(a_1 - ia_2)e^{i\omega t}. \quad (1.3.70)$$

It is then a simple matter, with these two conditions, to solve equations (1.3.66) to (1.3.68). The result is

$$\rho_{11} - \rho_{22} = (\rho_{11}^e - \rho_{22}^e) \frac{1 + T_2^2(\omega - \omega_0)^2}{1 + T_2^2(\omega - \omega_0)^2 + S} \quad (1.3.71)$$

$$a_1 - ia_2 = -(\rho_{11}^e - \rho_{22}^e)T_2 \frac{\omega_1 T_2(\omega - \omega_0) + i\omega_1}{1 + T_2^2(\omega - \omega_0)^2 + S} \quad (1.3.72)$$

where T_1 and T_2 stand for $1/\gamma_1$ and $1/\gamma_2$ respectively. S stands for the saturation factor defined as

$$S = \frac{g_S^2 \mu_B^2}{\hbar^2} \frac{B_1^2}{4} T_1 T_2 = \omega_1^2 T_1 T_2 \quad (1.3.73)$$

or

$$S = \gamma_s^2 B_1^2 T_1 T_2 / 4 \quad (1.3.74)$$

and ω_0 is now the new perturbed resonance frequency defined as

$$\omega_0 = \omega_{12} - \Delta\omega. \quad (1.3.75)$$

The presence of the factor $\frac{1}{4}$ is due to the fact that we have taken, as before, a linearly polarised field B_{RF} of the form

$$B_{RF} = iB_1 \cos \omega t. \quad (1.3.76)$$

In magnetic resonance theory it is standard practice to use a field with B_{RF} twice the value we have used here giving thus a circularly polarised component equal to B_1 . In the above expression γ_s is equal to $\mu_B g_s / \hbar$, or e/m for the electronic spin.

The two equations for $\rho_{11} - \rho_{22}$ and ρ_{12} give us ρ in the steady state. The average value of the components of the magnetisation can be calculated in the same way as we have done in §1.3.3 with the help of equation (1.3.45). We define

$$M_0 = -\frac{1}{2}N g_s \mu_B (\rho_{11}^e - \rho_{22}^e) \quad (1.3.77)$$

$$\chi_0 = M_0 / B_0. \quad (1.3.78)$$

For the components $\langle M_z \rangle$ and $\langle M_x \rangle$ we obtain

$$\langle M_z \rangle = \chi_0 B_0 \frac{1 + T_2^2(\omega - \omega_0)^2}{1 + T_2^2(\omega - \omega_0)^2 + S} \quad (1.3.79a)$$

$$\langle M_x \rangle = \frac{1}{2} \chi_0 B_0 \gamma_s T_2 \frac{-T_2(\omega - \omega_0) B_1 \cos \omega t + B_1 \sin \omega t}{1 + T_2^2(\omega - \omega_0)^2 + S}. \quad (1.3.79b)$$

A similar expression is obtained for $\langle M_y \rangle$. We define the RF susceptibility as†

$$\chi = \chi' + i\chi'' \quad (1.3.80)$$

and

$$\langle M_x \rangle = \chi' B_1 \cos \omega t + \chi'' B_1 \sin \omega t \quad (1.3.81)$$

$$\chi' = \frac{1}{2} \chi_0 B_0 \gamma_s T_2 \frac{-T_2(\omega - \omega_0)}{1 + T_2^2(\omega - \omega_0)^2 + S} \quad (1.3.82a)$$

$$\chi'' = \frac{1}{2} \chi_0 B_0 \gamma_s T_2 \frac{1}{1 + T_2^2(\omega - \omega_0)^2 + S}. \quad (1.3.82b)$$

A graphical representation of χ' and χ'' is shown in figure 1.3.2. This

† This form of χ is compatible with the fact that we have selected the clockwise rotating component of the field.

analysis is essentially that developed by Bloch (1946) in the context of magnetic resonance. χ' and χ'' are Bloch susceptibilities. In equation (1.3.81) it is observed that $\langle M_x \rangle$ is composed of a component in phase and a component in quadrature with the field. The component in phase is proportional to χ' and gives rise to dispersion phenomena. In frequency standards, it is a cause of frequency shifts. It is introduced by the real part of equation (1.3.72). The term out of phase, or in quadrature, is proportional to χ'' and is introduced by the imaginary part of equation (1.3.72). This term is responsible for either absorption or amplification. Another point is made explicit by these equations. It is observed that the value of χ'' is maximum for $\omega = \omega_0$, the resonant frequency, but that the resonance phenomenon is distributed over a certain bandwidth. This effect is caused by the relaxation phenomena.

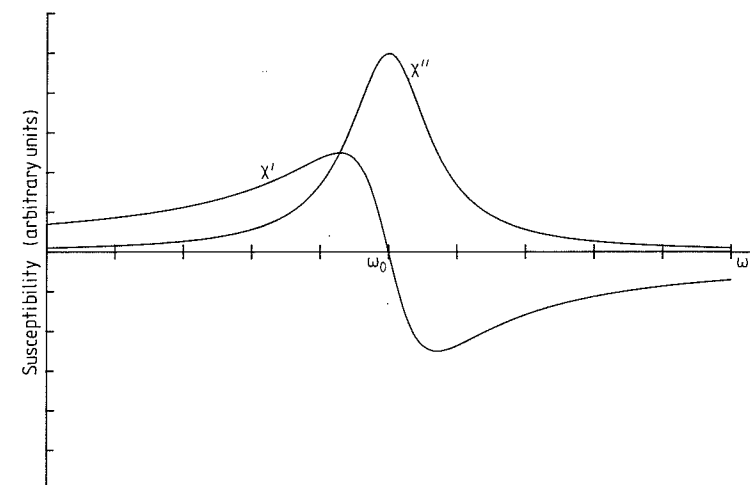


Figure 1.3.2 Graphical representation of the RF susceptibilities χ' and χ'' .

In the case that the applied field is weak, we may have

$$\frac{1}{4} \gamma_s^2 B_1^2 T_1 T_2 \ll 1$$

and the resonance has a line shape given by

$$g(v) = \frac{2 T_2}{1 + 4\pi^2 T_2^2 (v - v_0)^2}. \quad (1.3.83)$$

This is a Lorentz line shape. It is normalised in such a way as to make

$$\int_{-\infty}^{\infty} g(v) dv = 1. \quad (1.3.84)$$

It is observed that the line width at half the height of the resonance line is

$$\Delta\nu = \frac{1}{\pi T_2} = \frac{\gamma_2}{\pi} \quad (1.3.85)$$

as illustrated in figure 1.3.3.

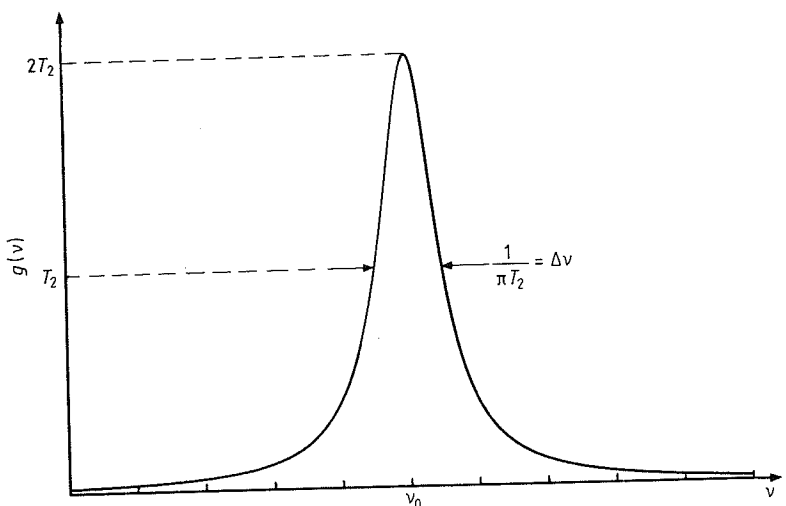


Figure 1.3.3 The Lorentz line shape (homogeneous broadening).

The concepts associated with this line shape are of the greatest importance for our main subject. In the case studied it was assumed that the magnetic moments were all perturbed equally in an average manner by the relaxation term. This made possible the introduction of a relaxation time T_2 and it is this term that gives rise to the Lorentz line shape. This type of interaction produces what is called homogeneous broadening. This is essentially caused by an interruption of the coherence in the ensemble by an interaction which acts on each individual magnetic moment. In other words, any sample of atoms in the ensemble is assumed to have the same resonant frequency and line as the ensemble itself and the system described by ρ is an exact representation of the average behaviour of the ensemble.

However, other causes of broadening may exist in the ensemble. For example, an inhomogeneous magnetic field may be present. In that case, groups of magnetic moments occupying different regions of space may have different resonant frequencies. They will give rise to an additional broadening to the one described above and this depends on

many factors such as the geometry and spatial coordinates. We call this effect inhomogeneous broadening. It is then necessary to describe the atomic ensemble by subensembles characterised by their own density matrix $\rho(\omega_0)$. Inhomogeneous broadening consequently depends on the type of perturbation and it is not possible to define, as in the homogeneous case, general parameters such as T_2 to characterise the process. In fact the line shape resulting from a given perturbation may not even, in some cases, be written in an analytical form since it depends on inhomogeneities whose distribution is unknown. We will have the occasion to come back to this point later. At the present time it is sufficient to say that an inhomogeneously broadened line is composed of several homogeneously broadened lines as shown in figure 1.3.4.

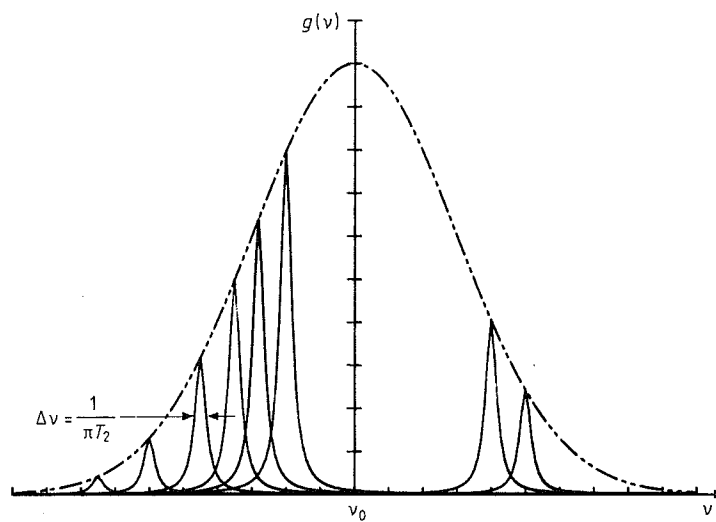


Figure 1.3.4 Illustration of inhomogeneous broadening. In the case shown it is assumed that the shape of the individual lines is Lorentzian.

The term S which we have called the saturation factor has important effects on the behaviour of the resonance line. When it is not small compared with one, its effect is first to broaden the resonance line. The homogeneous line shape is then given by

$$g(v, S) = \frac{2T_2(1 + S)^{1/2}}{1 + 4\pi^2 T_2^2(v - v_0)^2 + S}. \quad (1.3.86)$$

The width at half the height of the resonance line is then given by

$$\Delta\nu = \frac{(1 + S)^{1/2}}{\pi T_2} \quad (1.3.87)$$

On the other hand it is observed that for S large compared with one, both the values of ρ_{12} and $\rho_{11} - \rho_{22}$ tend to zero. The populations tend to equalise. The line becoming very broad, the coherence in the ensemble, measured by ρ_{12} , tends to become negligible. This is another important consideration in relation to atomic frequency standards. In some frequency standards, an electromagnetic field is applied to interrogate the atoms. This field, however, should not be too large, otherwise broadening and saturation effects such as those described above will become important.

It is readily noted that homogeneously and inhomogeneously broadened lines do not saturate in the same way. For example, in the second case, a field applied at frequency ν_1 may saturate the system only over a band of width $1/\pi T_2$ around ν_1 . It is then said that a hole is burned in the inhomogeneously broadened line.

(B) Dynamical solution

In this case we have to solve equations (1.3.66) to (1.3.68) with time as a variable. This cannot be done simply. However, at this time we would like to bring out only a few basic concepts and these can be obtained by making a few approximations. First, we make $\rho_{11}^e = \rho_{22}^e = \frac{1}{2}$ which means that the populations at equilibrium are equal. Second, we assume that the applied field has a frequency equal to the resonance frequency ω_0 . In such a case our two equations reduce to

$$\frac{d}{dt}(\rho_{11} - \rho_{22}) = -\gamma_1(\rho_{11} - \rho_{22}) - \omega_1 a_2 \quad (1.3.88)$$

$$\frac{d}{dt}(a_1 - ia_2) = -\gamma_2(a_1 - ia_2) - i\omega_1(\rho_{11} - \rho_{22}). \quad (1.3.89)$$

The solution of these two equations is given in Appendix 1D assuming $2\omega_1 > |\gamma_2 - \gamma_1|$. The result is

$$a_2 = [(\rho_{11} - \rho_{22})_0 \omega_1 / r] \{ \exp[-\frac{1}{2}(\gamma_1 + \gamma_2)t] \} \sin rt \quad (1.3.90)$$

$$\rho_{11} - \rho_{22} = (\rho_{11} - \rho_{22})_0 \exp[-\frac{1}{2}(\gamma_1 + \gamma_2)t] \left(\cos rt + \frac{\gamma_2 - \gamma_1}{2r} \sin rt \right) \quad (1.3.91)$$

where

$$r = [\omega_1^2 - \frac{1}{4}(\gamma_2 - \gamma_1)^2]^{1/2} \quad (1.3.92)$$

and $(\rho_{11} - \rho_{22})_0$ is the value of $\rho_{11} - \rho_{22}$ at time $t = 0$. Equations (1.3.90) and (1.3.91) take a very simple form in the case $\gamma_2 = \gamma_1 = \gamma$.

We then have

$$a_2 = (\rho_{11} - \rho_{22})_0 [\exp(-\gamma t)] \sin \omega_1 t \quad (1.3.93)$$

$$\rho_{11} - \rho_{22} = (\rho_{11} - \rho_{22})_0 [\exp(-\gamma t)] \cos \omega_1 t \quad (1.3.94)$$

and $\frac{1}{2}\pi$ as well as π pulses keep the same meaning as that given earlier. The main difference is that for a $\frac{1}{2}\pi$ pulse, the magnetisation cannot be tipped entirely in the xy plane since it is proportional to $(\rho_{11} - \rho_{22})_0 \exp(-\gamma t_p)$ where t_p is the length of the pulse. However, B_1 can generally be made large, making possible short t_p . In such a case the magnetisation can be tipped very nearly completely in the xy plane.

The variables under study in atomic frequency standards are not exactly those studied above. Nevertheless, it is possible to introduce a new concept, that of the 'fictitious spin', which allows the transposition of most of the physical interpretation we have made up to now on an ensemble of real spins, to ensembles of more complex systems. This is what we shall do next.

1.3.6 The Fictitious Spin

In the case of transitions among hyperfine levels, the actual motion of the electron and nuclear magnetic moments is quite complicated and cannot be described directly in terms as simple as those used up to now. For this reason we shall introduce the concept of the fictitious spin which will allow us even in the case of hyperfine interaction to describe the dynamics of the atomic ensemble with concepts developed so far.

Let us first introduce the four following matrices

$$I = \begin{pmatrix} 1 & 0 \\ 0 & 1 \end{pmatrix}, \sigma_1 = \begin{pmatrix} 0 & 1 \\ 1 & 0 \end{pmatrix}, \sigma_2 = \begin{pmatrix} 0 & -i \\ i & 0 \end{pmatrix}, \sigma_3 = \begin{pmatrix} 1 & 0 \\ 0 & -1 \end{pmatrix}. \quad (1.3.95)$$

The first one is recognised as the unity matrix while the three others are the Pauli matrices. These matrices form an orthogonal set. They have the following properties (Feynman *et al* 1965, chapter II):

$$\sigma_i \sigma_j = I \delta_{ij}, \text{Tr } \sigma_i = 0, \text{Tr}(\sigma_i \sigma_j) = 2\delta_{ij}, \det \sigma_i = -1, \quad (1.3.96)$$

$$[\sigma_i, \sigma_j] = 2i\sigma_k \quad (1.3.97)$$

where i, j and k take the values 1, 2 and 3 and form a cyclic permutation. These matrices form a complete set and any 2×2 matrices can be written as a linear superposition of them.

In many cases that we shall consider in this monograph, only two levels, out of a manifold which may contain many distinct levels, are affected by the applied perturbations. In such a case the interaction Hamiltonian and the density matrix can be represented by 2×2

resonance line width. The resulting AC signal is detected with a synchronous detector (lock-in) whose output is approximately the derivative of the absorption line. This forms a discriminator signal, which after integration is then used to lock the frequency of the interrogating microwave oscillator to the ^{87}Rb absorption line.

The hyperfine filter shown in figure 7.1.1 and discussed above is optional in the sense that filtering can be done inside the absorption cell by using natural rubidium. This last technique is called the integrated filter technique (IFT), while the configuration described previously is called the separated filter technique (SFT). Both techniques are described below and their advantages and disadvantages are discussed in detail.

7.1.2 The Resonance Signal

(A) Hypothesis

In order to obtain equations in an analytic form for the behaviour of the atomic ensemble, we introduce the following model (Vanier 1968).

(1) We assume that nitrogen or a mixture of nitrogen and another gas is used in the resonance cell.

(2) There is no scattered light re-emitted by the system when the atoms, after being pumped to the P state, fall back to the ground state. The energy is completely absorbed by the nitrogen molecules during nitrogen-rubidium collisions (Happer 1972).

(3) There is equal probability for all atoms to fall into any of the levels of the ground state after the optical pumping cycle. We make this last simplification because of our lack of knowledge of the exact mechanism of energy transfer from the excited rubidium atoms to the nitrogen buffer gas during collisions.

(4) In the absence of light, thermal relaxation gives equal probability of occupation of the eight ground-state sublevels. The important relaxation mechanisms which are present include wall collisions, spin-exchange collisions and buffer gas collisions (binary type). These relaxation processes have been studied in some detail in chapter 3. It would be extremely difficult to take them all into account separately. In practice, it is best to characterise the relaxation of the population of any levels by the rate γ_1 and the relaxation of the hyperfine coherence by the rate γ_2 . These rates are then the combined effect of all mechanisms of relaxation. We do not expect much of an error in doing this and the simplification which is obtained in the solution of the equations is rather important. Otherwise the problem would be extremely hard, if not impossible, to treat analytically.

(B) Rate equations

The energy levels involved in the following calculation are shown in

figure 7.1.5. Microwave radiation is applied to the system at a frequency corresponding to the transition between levels 3 and 7 and we assume that coherence exists only between these two levels.

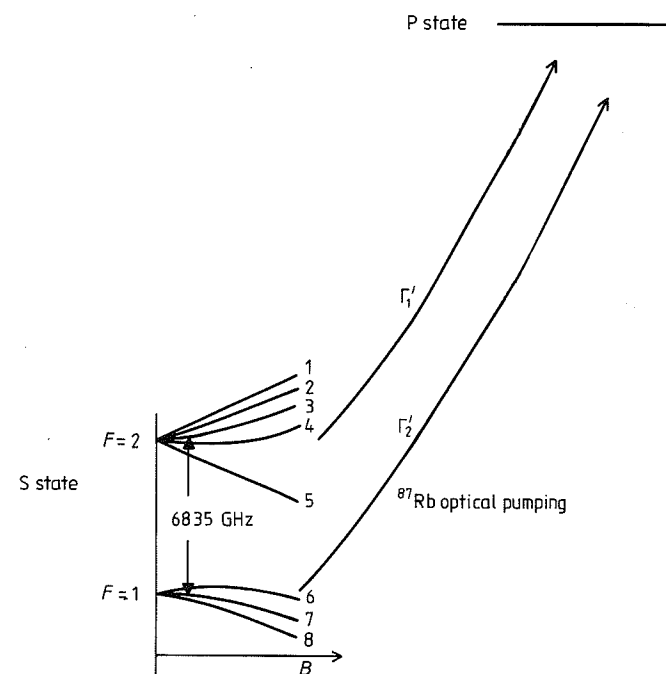


Figure 7.1.5 Simplified energy level manifold used in the calculation of the optical pumping of ^{87}Rb .

The density matrix in this case is

$$\rho = \begin{pmatrix} \rho_{11} & 0 & 0 & 0 & 0 & 0 & 0 & 0 \\ 0 & \rho_{22} & 0 & 0 & 0 & 0 & 0 & 0 \\ 0 & 0 & \rho_{33} & 0 & 0 & 0 & 0 & \rho_{73} \\ 0 & 0 & 0 & \rho_{44} & 0 & 0 & 0 & 0 \\ 0 & 0 & 0 & 0 & \rho_{55} & 0 & 0 & 0 \\ 0 & 0 & 0 & 0 & 0 & \rho_{66} & 0 & 0 \\ 0 & 0 & \rho_{37} & 0 & 0 & 0 & \rho_{77} & 0 \\ 0 & 0 & 0 & 0 & 0 & 0 & 0 & \rho_{88} \end{pmatrix}. \quad (7.1.1)$$

The various contributions to the rate equations are not correlated and they can be added directly:

$$\frac{d\rho}{dt} = \left(\frac{d\rho}{dt} \right)_{\text{OP}} + \left(\frac{d\rho}{dt} \right)_{\text{rel}} + \left(\frac{d\rho}{dt} \right)_{\text{rad}} \quad (7.1.2)$$

where $(d\rho/dt)_{OP}$, $(d\rho/dt)_{rel}$ and $(d\rho/dt)_{rad}$ are the effects of optical pumping, relaxation and microwave radiation respectively on the evolution of the density matrix ρ .

(1) Optical pumping

The lamps normally used are operated in a condition such that the lines are broad with respect to the Zeeman splitting of a hyperfine level of the ground state. We call Γ'_1 the pumping rate from the levels 1, 2, 3, 4 and 5 to the excited P state and Γ'_2 the pumping rate from the levels 6, 7 and 8 to the same excited state. We have

$$\Gamma'_i = \int_0^\infty \mathcal{J}_i(v) \sigma_i(v) dv \quad i = 1, 2 \quad (7.1.3)$$

where $\mathcal{J}_i(v)$ is the photon flux per unit frequency interval per unit area at the frequency v and $\sigma_i(v)$ is the effective cross section for absorption of a photon by an atom at frequency v . The values of $\mathcal{J}_i(v)$ and thus Γ'_i are functions of the coordinates x , y and z . From the analysis made in §4.2 and from the hypothesis made above, the rate equations for optical pumping can be written as

$$\left(\frac{d\rho_{\mu\mu}}{dt} \right)_{OP} = -\Gamma'_i \rho_{\mu\mu} + \frac{\Gamma'_1 \sum_{\mu'=1}^5 \rho_{\mu'\mu'} + \Gamma'_2 \sum_{\mu'=6}^8 \rho_{\mu'\mu'}}{8}. \quad (7.1.4)$$

Here $i = 1$ for $\mu = 1, 2, 3, 4, 5$, $i = 2$ for $\mu = 6, 7, 8$ and

$$\left(\frac{d\rho_{73}}{dt} \right)_{OP} = -\left(\frac{\Gamma'_1 + \Gamma'_2}{2} + i\Delta\omega_l \right) \rho_{73} \quad (7.1.5)$$

where $\Delta\omega_l$ is the light shift.

(2) Relaxation

According to hypothesis (4), uniform relaxation is assumed with equal populations in the ground-state sublevels at equilibrium. Such an assumption means that the slight difference in population of the levels at the temperature of operation, T , is negligible according to the Boltzmann law of equilibrium, compared with the population differences created by the optical pumping process. It also means that we do not take into account the slight difference that may exist in the relaxation rates associated with various pairs of levels and whose origin could be buffer gas collisions, spin-exchange interactions or wall collisions. The rate equations for relaxation are thus written simply as

$$\left(\frac{d\rho_{\mu\mu}}{dt} \right)_{rel} = \gamma_1 (\frac{1}{8} - \rho_{\mu\mu}) \quad \left(\frac{d\rho_{\mu\mu'}}{dt} \right)_{rel} = -\gamma_2 \rho_{\mu\mu'} \quad \text{for } \mu \neq \mu' \quad (7.1.6)$$

where γ_1 and γ_2 are the relaxation rates of the population and the coherence respectively. These relaxation rates include the effects of all relaxation mechanisms that may be present.

Theory

(3) Microwave radiation

The microwave radiation is applied between levels 3 and 7 and it contributes to the rate equations as described in §1.2.4. It follows that

$$\left(\frac{d\rho_{33}}{dt} \right)_{rad} = b \operatorname{Im}[\rho_{73} \exp(-i\omega t)] \quad (7.1.7)$$

where b is evaluated from equation (1.2.66) and table 1.2.1. It is given by

$$b = \mu_B B_z / \hbar \quad (7.1.8)$$

where B_z is the amplitude of the RF field induction parallel to the static field at the site of a given atom in the cell. ω is the angular frequency of the applied microwave radiation. The other equations are

$$\left(\frac{d\rho_{77}}{dt} \right)_{rad} = -b \operatorname{Im}[\rho_{73} \exp(-i\omega t)] \quad (7.1.9)$$

$$\left(\frac{d\rho_{73}}{dt} \right)_{rad} = -i \frac{b}{2} (\rho_{33} - \rho_{77}) \exp(i\omega t) + i(\omega_0 - \Delta\omega_l) \rho_{73} \quad (7.1.10)$$

$$\left(\frac{d\rho_{\mu\mu}}{dt} \right)_{rad} = 0 \quad \text{for } \mu \neq 3 \text{ and } \mu \neq 7. \quad (7.1.11)$$

(C) Solution of the system of rate equations

Replacing the various $d\rho/dt$ in equation (7.1.2) by the expressions just derived, we obtain a set of nine differential equations, eight for the diagonal elements and one for the off-diagonal element. This set of equations is solved at equilibrium. It is recalled that, as in the case of the two-level system discussed in §4.2.5, the pumping rates, the RF field and the density matrix elements are all functions of the position in the resonance cell. The solution obtained is thus valid locally.

The off-diagonal element oscillates at the frequency of the RF field and is set equal to

$$\rho_{73} = \frac{1}{2}(a_1 - ia_2)e^{i\omega t}. \quad (7.1.12)$$

Substituting in equation (7.1.10), one obtains

$$\operatorname{Im}(\rho_{73} e^{-i\omega t}) = -\frac{1}{2}a_2 = \frac{1}{2}bd(\rho_{33} - \rho_{77}) \quad (7.1.13)$$

where

$$d = \left(\frac{\Gamma'_1 + \Gamma'_2}{2} + \gamma_2 \right) / \left[(\omega - \omega')^2 + \left(\frac{\Gamma'_1 + \Gamma'_2}{2} + \gamma_2 \right)^2 \right] \quad (7.1.14)$$

and

$$\omega' = \omega_0 - \Delta\omega_l. \quad (7.1.15)$$

Symmetry in the rate equations for the diagonal terms leads to the

relation

$$\rho_{11} = \rho_{22} = \rho_{44} = \rho_{55} \quad \rho_{66} = \rho_{88}. \quad (7.1.16)$$

The number of unknown diagonal elements is reduced to four by means of this equation. They are ρ_{11} , ρ_{33} , ρ_{66} and ρ_{77} . A steady-state solution is assumed for which

$$d\rho_{\mu\mu}/dt = 0 \quad \text{for } \mu = 1, \dots, 8 \quad (7.1.17)$$

and a set of equations is obtained which can be written in the matrix form

$$\begin{pmatrix} \frac{1}{2}\Gamma'_1 & \frac{1}{8}\Gamma'_1 & -\frac{3}{4}\Gamma'_2 - \gamma_1 & \frac{1}{8}\Gamma'_2 \\ -\frac{1}{2}\Gamma'_1 - \gamma_1 & \frac{1}{8}\Gamma'_2 & \frac{1}{4}\Gamma'_2 & \frac{1}{8}\Gamma'_2 \\ \frac{1}{2}\Gamma'_1 & -\frac{17}{8}\Gamma'_1 - \gamma_1 - \frac{1}{2}b^2d & \frac{1}{4}\Gamma'_2 & \frac{1}{8}\Gamma'_2 + \frac{1}{2}b^2d \\ \frac{1}{2}\Gamma'_1 & \frac{1}{8}\Gamma'_1 + \frac{1}{2}b^2d & \frac{1}{4}\Gamma'_2 & -\frac{7}{8}\Gamma'_2 - \gamma_1 - \frac{1}{2}b^2d \end{pmatrix} \times \begin{pmatrix} \rho_{11} \\ \rho_{33} \\ \rho_{66} \\ \rho_{77} \end{pmatrix} = -\frac{1}{8}\gamma_1 \times \begin{pmatrix} 1 \\ 1 \\ 1 \\ 1 \end{pmatrix}. \quad (7.1.18)$$

We are interested in the photon flux at position z_0 , i.e. at the exit of the cell†. In an analysis similar to that done in §4.2.5 in which the parameters are assumed to be functions of the light frequency and the z coordinate only, one has

$$\mathcal{J}(\nu, z_0) = \mathcal{J}(\nu, 0) \exp\{-nz_0[\sigma_1(\nu)\langle n_1 \rangle + \sigma_2(\nu)\langle n_2 \rangle]\} \quad (7.1.19)$$

where n is the rubidium vapour density in the cell. n_1 and n_2 are the sum of the density matrix diagonal elements in each hyperfine level:

$$\begin{aligned} n_1 &= \rho_{11} + \rho_{22} + \rho_{33} + \rho_{44} + \rho_{55} \\ n_2 &= \rho_{66} + \rho_{77} + \rho_{88}. \end{aligned} \quad (7.1.20)$$

The average of n_1 and of n_2 is taken over the length of the cell. It is possible to transform equation (7.1.18) in such a way that the terms n_1 , n_2 , ρ_{11} and ρ_{66} are the unknowns (Missout 1974, Missout and Vanier 1975). A new inverse matrix is obtained, of which only two lines are necessary since only n_1 and n_2 are required in the calculation. The result is

$$n_1 = A_1/D \quad n_2 = A_2/D \quad (7.1.21)$$

†In the analysis we do not take into account the variation of quantities such as the microwave field, the pumping rates and the relaxation rates with the radial distance from the system's axis of symmetry. For a consideration of some of the inhomogeneities created by such variations the reader is referred to Tremblay *et al* (1985).

where

$$\begin{aligned} A_1 &= 5(\Gamma'_1 + \gamma_1)(\Gamma'_2 + \gamma_1)^2 \\ &\quad + b^2d(3\Gamma'_1\Gamma'_2 + 3\Gamma'_1\gamma_1 + 7\Gamma'_2\gamma_1 + 5\gamma_1^2 + 2\Gamma'_2)^2 \end{aligned} \quad (7.1.22)$$

$$\begin{aligned} A_2 &= 3(\Gamma'_1 + \gamma_1)^2(\Gamma'_2 + \gamma_1) \\ &\quad + b^2d(2\Gamma'_1\Gamma'_2 + 4\Gamma'_1\gamma_1 + 2\Gamma'_2\gamma_1 + 3\gamma_1^2 + \Gamma'_1)^2 \end{aligned} \quad (7.1.23)$$

$$\begin{aligned} D &= (5\Gamma'_2 + 3\Gamma'_1 + 8\gamma_1)(\Gamma'_1 + \gamma_1)(\Gamma'_2 + \gamma_1) \\ &\quad + b^2d(5\Gamma'_1\Gamma'_2 + 2\Gamma'_2^2 + \Gamma'_1^2 + 7\Gamma'_1\gamma_1 + 9\Gamma'_2\gamma_1 + 8\gamma_1^2). \end{aligned} \quad (7.1.24)$$

By simple algebraic manipulation, n_1 and n_2 can then be written

$$n_1 = n_{10} + \frac{b^2(q - gn_{10})n_{10}/5(\Gamma'_1 + \gamma_1)(\Gamma'_2 + \gamma_1)^2\gamma'_2}{1 + S + (\omega - \omega')^2/(\gamma'_2)^2} \quad (7.1.25)$$

$$n_2 = n_{20} + \frac{b^2(p - gn_{20})n_{20}/3(\Gamma'_1 + \gamma_1)^2(\Gamma'_2 + \gamma_1)\gamma'_2}{1 + S + (\omega - \omega')^2/(\gamma'_2)^2} \quad (7.1.26)$$

where

$$n_{10} = 5(\Gamma'_2 + \gamma_1)/(5\Gamma'_2 + 3\Gamma'_1 + 8\gamma_1) \quad (7.1.27)$$

$$n_{20} = 3(\Gamma'_1 + \gamma_1)/(5\Gamma'_2 + 3\Gamma'_1 + 8\gamma_1) \quad (7.1.28)$$

$$S = b^2/\gamma'_1\gamma'_2 \quad (7.1.29)$$

$$\gamma'_1 = (\Gamma'_1 + \gamma_1)(\Gamma'_2 + \gamma_1)(5\Gamma'_2 + 3\Gamma'_1 + 8\gamma_1)/g \quad (7.1.30)$$

$$\gamma'_2 = (\Gamma'_1 + \Gamma'_2)/2 + \gamma_2 \quad (7.1.31)$$

$$p = 2\Gamma'_1\Gamma'_2 + 4\Gamma'_1\gamma_1 + 2\Gamma'_2\gamma_1 + 3\gamma_1^2 + \Gamma'_1^2 \quad (7.1.32)$$

$$q = 3\Gamma'_1\Gamma'_2 + 3\Gamma'_1\gamma_1 + 7\Gamma'_2\gamma_1 + 5\gamma_1^2 + 2\Gamma'_2^2 \quad (7.1.33)$$

$$g = 5\Gamma'_1\Gamma'_2 + 2\Gamma'_2^2 + \Gamma'_1^2 + 7\Gamma'_1\gamma_1 + 9\Gamma'_2\gamma_1 + 8\gamma_1^2. \quad (7.1.34)$$

n_{10} and n_{20} are the equilibrium fractional populations of the two hyperfine levels when the microwave radiation is absent i.e. when we have $b = 0$.

(D) The resonance signal

The characteristics of the resonance signal are calculated as in §4.2.5 by means of equation (7.1.19).

(1) The cross section $\sigma_i(\nu)$

An expression for $\sigma_i(\nu)$ can be obtained from a calculation using equation (4.2.199). Using the relation

$$\mathcal{J}(\nu) = \frac{2\pi}{\hbar\omega} I(\omega) \quad (7.1.35)$$

the transition probability becomes

$$P_{F_g m_g \rightarrow F_e m_e} = \frac{3\pi c^2}{2\omega^2} \mathcal{J}(\nu) (2F_g + 1)(2F_e + 1)(2J_e + 1) \times \left(\begin{array}{ccc} F_e & 1 & F_g \\ -m_e & q & m_g \end{array} \right)^2 \times \left\{ \begin{array}{ccc} F_e & 1 & F_g \\ J_g & I & J_e \end{array} \right\}^2 \times \frac{1}{\tau} \quad (7.1.36)$$

where the terms are defined in §4.2.6.

In the present study, $\mathcal{J}(\nu)$ is the photon flux associated with a D_1 or a D_2 line and is assumed to have a broad spectrum. Pumping is thus done from all levels of a given hyperfine state F_g to all levels of either excited state $P_{1/2}$ or $P_{3/2}$. Consequently, an average is made over all starting levels m_g of F_g followed by a summation over all levels in either of the P states. Using the properties of sum rules on $3j$ and $6j$ symbols (Judd 1963), the transition probability becomes

$$P_{m_g \rightarrow J_e} = \frac{3\pi c^2}{2\omega^2} \frac{2J_e + 1}{2J_g + 1} \frac{\mathcal{J}(\nu)}{\tau} k_\lambda. \quad (7.1.37)$$

where J_e is the total angular momentum of the excited state. The factor k_λ is introduced to take into account the number of polarisation components present in $\mathcal{J}(\nu)$. If $\mathcal{J}(\nu)$ is isotropic and not polarised, $k_\lambda = 1$. In the rubidium frequency standard the light beam is unpolarised and propagates along the axis of the magnetic field. The polarisation is then called σ and k_λ is $\frac{2}{3}$. The pumping rate can then be written

$$\Gamma'_u = \int_{-\infty}^{\infty} \frac{\pi c^2}{\omega^2} \frac{2J_e + 1}{2J_g + 1} \frac{\mathcal{J}(\nu)}{\tau} g_a(\nu) d\nu \quad (7.1.38)$$

where $g_a(\nu)$ is the normalised absorption line shape. A comparison with equation (7.1.3) then gives

$$\sigma(\nu) = \frac{\pi c^2}{\omega^2} \frac{2J_e + 1}{2J_g + 1} \frac{g_a(\nu)}{\tau} = \sigma_0 g_a(\nu). \quad (7.1.39)$$

The cross section is independent of the ground-state level considered. However, it depends on ν and we have

$$\sigma_1(\nu) \neq \sigma_2(\nu). \quad (7.1.40)$$

If the adsorption line shape is assumed to be Gaussian as described by equation (3.2.29), the cross section for the absorption of D_1 radiation, σ polarisation is given by

$$\sigma(\nu) = \frac{\pi^{1/2} c^2}{\omega^2 \tau} \frac{2(\ln 2)^{1/2}}{\Delta \nu_a} \exp[-(4\ln 2)(\nu - \nu_0)^2 / (\Delta \nu_a)^2] \quad (7.1.41)$$

where $\Delta \nu_a$ is the absorption line width given by equation (3.2.30). It is 527 MHz at 60 °C. At the line centre the cross section is

$$\sigma(\nu_0) = 3.10 \times 10^{-15} \text{ m}^2 \quad (D_1; \sigma \text{ polarisation}).$$

The cross section for D_2 , σ polarisation is calculated in the same way. It is

$$\sigma(\nu_0) = 6.48 \times 10^{-15} \text{ m}^2 \quad (D_2; \sigma \text{ polarisation}).$$

(2) The relative importance of D_1 and D_2 pumping

In practice, optical pumping is done with resonance lamps emitting both D_1 and D_2 radiation, and equation (7.1.19) applies to the two hyperfine components of both D_1 and D_2 lines. However, it is found experimentally that the optical pumping is done mostly with the D_1 line. As will be seen in §7.3, this is due to the fact that the hyperfine filter is more efficient with the D_1 line than with the D_2 line. Actually, at the temperature where the undesired component of the D_1 line (cd in figure 7.1.2(b)) is absorbed, both components of the D_2 line (ihg and lkj in figure 7.1.2(a)) are greatly reduced. At the normal temperature of operation it is expected that the D_2 line intensity at the output of the hyperfine filter is of the order of 30% of the D_1 line intensity (Busca *et al* 1973). Furthermore, as seen in the previous section, the cross section $\sigma(\nu_0)$ is twice as large for the D_2 line as for the D_1 line. It will be shown below that the resonance signal is proportional to the pumping rates at position z_0 as in the case of the two-level system studied in §4.2.5. These rates have an exponential dependence on z similar to that shown in equation (7.1.19) and it follows that the signal due to the D_2 line is much attenuated compared with that due to the D_1 line. Consequently the contribution of the D_2 pumping to the signal will be neglected. In practice, however, the D_2 radiation may contribute to an added relaxation and broadening of the resonance line.

(3) The line shape

Within this approximation, the light transmitted as given by equation (7.1.19) is

$$\mathcal{J}_t(\nu, z_0) = \mathcal{J}(\nu, 0) \exp\{-nz_0[\sigma_1(\nu)\langle n_1 \rangle + \sigma_2(\nu)\langle n_2 \rangle]\} \quad (7.1.42)$$

Using the values of n_1 and n_2 calculated above, one obtains

$$\begin{aligned} \mathcal{J}_t(\nu, z_0) = \mathcal{J}(\nu, z) \exp\{ & -nz_0[\sigma_1(\nu)\langle n_{10} \rangle \\ & - \left(k \frac{S}{S+1} \frac{\lambda/2\gamma'_1}{1 + (\omega - \omega_0)^2/(\gamma'_2)^2(S+1)} \right) \} + \sigma_2(\nu)\langle n_{20} \rangle \\ & + \left(k \frac{S}{S+1} \frac{\lambda/2\gamma'_1}{1 + (\omega - \omega_0)^2/(\gamma'_2)^2(S+1)} \right) \} \}. \end{aligned} \quad (7.1.43)$$

This can be written

$$\mathcal{I}_t(v, z_0) = \mathcal{I}(v, z_0) \times \exp\left(-nz_0 \left(k \frac{S}{S+1} \frac{\lambda/2\gamma'_1}{1 + (\omega - \omega_0)^2/(\gamma'_2)^2(S+1)} \right) [\sigma_2(v) - \sigma_1(v)]\right) \quad (7.1.44)$$

where

$$\mathcal{I}(v, z_0) = \mathcal{I}(v, 0) \exp\{-nz_0[\langle n_{10} \rangle \sigma_1(v) + \langle n_{20} \rangle \sigma_2(v)]\} \quad (7.1.45)$$

is the residual light intensity at frequency v and position z_0 in the absence of RF fields. The factor k is defined as

$$k = 16(\Gamma'_1 + \gamma_1)(\Gamma'_2 + \gamma_1)(\Gamma'_1\Gamma'_2 + \Gamma'_2\gamma_1 + \Gamma'_1\gamma_1 + \gamma_1^2)/g^2 \quad (7.1.46)$$

and λ is defined by equation (4.2.164), as $(\Gamma'_2 - \Gamma'_1)/2$. Equation (7.1.43) is very similar to that obtained in §4.2.5 for a two-level system. The difference resides in the presence of the factor k in the resonant term and in the definition of the various parameters, γ'_1 , γ'_2 and S , which take more complicated forms due to the fact that we deal with an eight-level system.

The resonance term is generally small. In practice a fractional resonance dip of a few per cent at maximum is observed. In such a case the exponential function can be expanded in series and an integration over the whole spectrum, using equation (7.1.3), gives the total photon flux transmitted as

$$\mathcal{I}_t(z_0) = \mathcal{I}_{10}(z_0) - nz_0\lambda(z_0) \left\langle k \frac{S}{S+1} \frac{\lambda/\gamma'_1}{1 + (\omega - \omega_0)^2/(\gamma'_2)^2(S+1)} \right\rangle \quad (7.1.47)$$

where $\mathcal{I}_{10}(z_0)$ is the flux of photons transmitted at position z_0 in the absence of RF radiation. According to the present analysis, the line shape is approximately Lorentzian only for very small signals. Even in that case the resonance is inhomogeneously broadened due to the fact that ω_0 and γ'_2 are both functions of the pumping rates, which vary with position in the cell. When the effect of the RF radiation on the hyperfine level population is large, the line shape appears to be a complicated function of many parameters, such as the pumping rates, the saturation factor and the frequency. It is thus expected that the resonance frequency observed in practice will be a function of the RF radiation power. Since, furthermore, the signal is detected by means of frequency modulation of the RF radiation, the resonance frequency observed will also depend on the index of modulation.

(E) Optimisation of the signal amplitude

The resonance signal amplitude as given by equation (7.1.47) can be optimised for various parameters. However, care must be taken in the

choice of the criteria for which this optimisation is sought. This is because operational constraints may dictate conflicting requirements.

(1) Pumping rate difference ' λ '

From the form of the equation it appears that the signal is greatest when λ is largest. This condition is fulfilled at optimum filtering and this happens at a relatively high temperature of the filter cell. However, this operating condition is not necessarily compatible with the condition of zero light shift, as will be shown in §7.3.2. Since this last condition is extremely important for long-term frequency stability, the filter cell is generally adjusted for zero light shift instead of maximum signal.

(2) Saturation factor

The condition of zero light shift is assumed. In such a case ω can be set equal to ω_0 and the signal amplitude is given by

$$\mathcal{I}_t(z_0) = \mathcal{I}_{10}(z_0) - nz_0\lambda(z_0) \left\langle k \frac{S}{S+1} \frac{\lambda}{\gamma'_1} \right\rangle. \quad (7.1.48)$$

The saturation factor S is a function of the RF field in the cavity. It is readily observed that the signal is maximum for $S \gg 1$. However, as will be seen in §7.2, the signal height is not itself the parameter to maximise. In practice the frequency ω is modulated at a relatively low frequency and an error signal is derived by means of a synchronous detector. This resulting signal has the shape of a discriminator pattern and is used to lock to the resonance the crystal oscillator from which the interrogation frequency is derived. It is obvious, as in the caesium frequency standard (see §5.5.2), that the important factor is the slope of the discriminator pattern close to the centre of the resonance line. It is found that the slope is maximum for $S = 2$ in the case of slow modulation. The reason for this behaviour is due to the fact that a large value of S produces a broad resonance line and decreases the slope of the discriminator pattern. In the analysis that follows, the saturation factor will be assumed to be equal to 2.

(3) Cell length

Assuming that the filter cell temperature has been set for minimum light shift, which means that the relative values of $\Gamma'_1(0)$ and $\Gamma'_2(0)$ have been fixed, equation (7.1.48) can in principle be optimised for maximum signal as a function of cell length. The weak dependence of the line width on the cell length, through the space-averaging process contained in equation (7.1.48), is not expected to be large and is neglected. Thus the slope of the discriminator pattern is expected to be a function of the signal height optimised as a function of the cell length.

The fractional signal amplitude is defined as

$$\alpha = \frac{\mathcal{I}_t(z_0) - \mathcal{I}_{i0}(z_0)}{\mathcal{I}_{i0}(z_0)} \quad (7.1.49)$$

which for $S = 2$ and $\omega = \omega_0$ gives

$$\alpha = -\frac{2}{3} \frac{nz_0\lambda(z_0)}{\mathcal{I}_{i0}(z_0)} \left(\frac{k\lambda}{\gamma'_1} \right). \quad (7.1.50)$$

In order to go further in the calculation, the actual line shape of $\mathcal{I}_i(v, 0)$ and $\sigma_i(v)$ must be made explicit. Both, in principle, are expected to be Gaussian, and calculations based on this hypothesis have been made in the past (Tessier and Vanier 1971b). In practice, however, the pumping lamp is operated at a temperature where self-reversal cannot be entirely neglected. This effect results in a flattening of the top of the optical lines. The hyperfine filter also causes a strong distortion of the various optical lines, with the consequence that the line shapes are very far from being Gaussian. Both effects are illustrated in figures 7.3.3 and 7.3.4 which will be used later to illustrate the light shift phenomenon.

Consequently, in order to simplify the calculation, the pumping and absorption lines are assumed to be both represented by rectangular spectra as illustrated in figure 7.1.6. Thus $\sigma_i(v) = \sigma_i(v_0)$ for v inside the band of frequencies $\Delta\nu_a$ centred on v_0 , the centre frequency of the absorption line, and $\sigma_i(v) = 0$ for v outside that band. $\Delta\nu_a$ is the Doppler width of the absorption line and is of the order of 500 MHz. In the same way $\mathcal{I}_i(v) = \mathcal{I}_i(v_0)$ for v inside a band of frequencies $\Delta\nu_l$ centred on the frequency at which the line height is maximum and $\mathcal{I}_i(v) = 0$ for v outside that band. $\Delta\nu_l$ is the width at half the height of the emission line of the lamp and is of the order of 1–1.5 GHz. Such approximations are quite drastic, but nevertheless they have been used in the past with relative success to calculate the light shift (Mathur *et al* 1968).

Within such approximations, and using equation (7.1.19), the photon flux at position z without an RF field applied is given by

$$\mathcal{I}_{i0}(z) = \mathcal{I}_{i0}(0) \left(1 - \frac{\Delta\nu_a}{\Delta\nu_l} \{ 1 - \exp[-nz\sigma(v_0)\langle n_{i0} \rangle] \} \right). \quad (7.1.51)$$

In the case of high densities or large values of z the exponential term can be neglected. In such a case the light transmitted is controlled by the ratio of the two widths involved.

On the other hand, as seen in figure 7.1.6, pumping is efficient only over the band $\Delta\nu_a$ where $\sigma(v) = \sigma(0)$. Using equation (7.1.3), the variation of Γ'_i with z is calculated as

$$\Gamma'_i(z) = \Gamma'_i(0) \exp[-nz\sigma(v_0)\langle n_{i0} \rangle] \quad (7.1.52)$$

where

$$\Gamma'_i(0) = \mathcal{I}_{i0}(0)\sigma(v_0)\Delta\nu_a/\Delta\nu_l \quad (7.1.53)$$

$\mathcal{I}_{i0}(0)$ being the total photon flux at the entrance of the cell. Equation (7.1.51) can then be written

$$\mathcal{I}_{i0}(z) = \frac{\Gamma'_i(0)}{\sigma(v_0)} \frac{\Delta\nu_l}{\Delta\nu_a} \left(1 - \frac{\Delta\nu_a}{\Delta\nu_l} \{ 1 - \exp[-nz\sigma(v_0)\langle n_{i0} \rangle] \} \right) \quad (7.1.54)$$

and the fractional signal height becomes

$$\alpha = -\frac{2}{3} \frac{y_0\lambda(z_0)}{\sum_{i=1}^2 \Gamma'_i(0) \{ 1 - (\Delta\nu_a/\Delta\nu_l)[1 - \exp(-y_0\langle n_{i0} \rangle)] \}} \frac{\Delta\nu_a}{\Delta\nu_l} \left(\frac{k\lambda}{\gamma'_1} \right) \quad (7.1.55)$$

where $\langle n_{i0} \rangle$ is an average over the whole cell. The parameter y_0 stands for

$$y_0 = n\sigma(v_0)z_0. \quad (7.1.56)$$

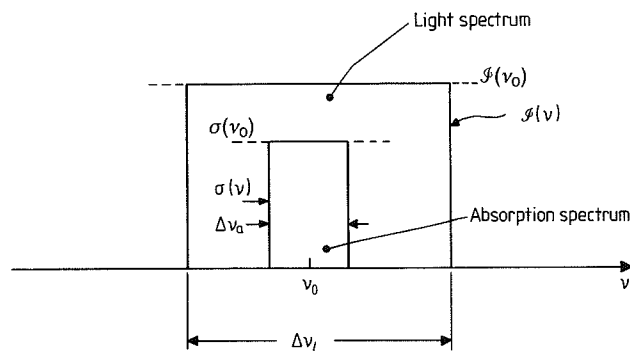


Figure 7.1.6 Approximate rectangular spectra representing the absorption in the cell and the light emission by the lamp.

In order to calculate $\lambda(z_0)$ by means of equation (7.1.53), the n_{i0} must be known. They are given by equations (7.1.27) and (7.1.28), which are functions of the pumping rates. Furthermore, the Γ'_i and n_{i0} are functions of position. Consequently, in order to obtain these various parameters, the cell is divided into thin slices and the equilibrium values of the n_{i0} are calculated for each successive slice using the Γ'_i at the output of one slice as the input pumping rate of the next slice. The actual resulting values of Γ'_i and n_{i0} for various values of the pumping rates are plotted in figures 7.1.7 and 7.1.8 as a function of y . The value of $k\lambda/\gamma'_1$ can then be calculated for the various slices and its average can be obtained as a function of the length y_0 considered. Then σ can be calculated. The results of this exercise are shown in figure 7.1.9.

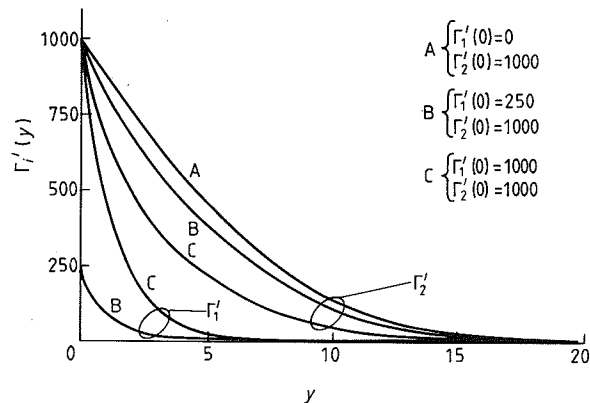


Figure 7.1.7 Variation of the pumping rates Γ'_1 and Γ'_2 with position in the cell for various conditions. The population relaxation rate is assumed to be equal to 300 s^{-1} .

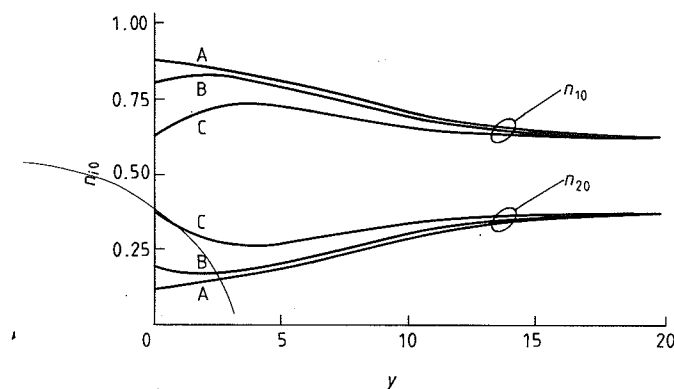


Figure 7.1.8 Variation of the population of the hyperfine levels with position in the cell for the same conditions as in figure 7.1.7.

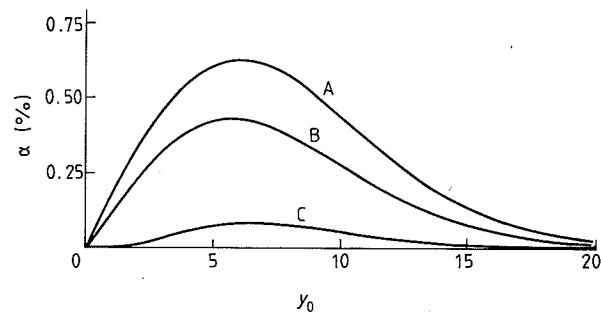


Figure 7.1.9 Amplitude of fractional signal height as a function of fractional cell length for the same conditions as in figure 7.1.7.

(4) Relaxation and line width

(a) *Longitudinal relaxation.* This rate, denoted γ_1 , as defined through the saturation factor is given by equation (7.1.30). It is a function of the pumping rates and of γ_1 , the population relaxation rate.

The value of γ_1 can be calculated from the analysis given in chapter 3 relative to relaxation. It is given by

$$\gamma_1 = \gamma_{1se} + \gamma_{lw} + \gamma_{1BG} \quad (7.1.57)$$

where γ_{1se} is the spin-exchange relaxation rate, γ_{lw} is the wall relaxation rate reduced by the diffusion process in the buffer gas and γ_{1BG} is the relaxation rate caused by collision with the buffer gas atoms.

The spin-exchange rate is given by equation (3.6.98):

$$\gamma_{1se} = n \bar{v}_r \sigma. \quad (7.1.58)$$

The density of rubidium can be obtained from the ideal gas law and the pressure-temperature relation (Killian 1926):

$$\log P = -\frac{4132}{T} + 7.43 \quad (7.1.59)$$

and

$$n = 9.656 \times 10^{18} P/T \quad (7.1.60)$$

where P is expressed in torr† and T in K. The density is then in atom cm^{-3} . The values of P and n in the range of temperature of interest in the present study are given in table 7.1.1.

At a temperature of 60°C the rubidium density is $3.05 \times 10^{11} \text{ cm}^{-3}$ and \bar{v}_r as given by equation (3B.12) is $4.01 \times 10^4 \text{ cm s}^{-1}$. The value of the spin-exchange cross section is taken from table 3.6.6. An average of the data from references d, g and i, for which the temperature of the measurement has been reported, is taken. As seen in table 3.6.4, the cross section is not expected to be a strong function of temperature in the range covered, and the scatter in the data is larger than the temperature-dependent changes expected. Thus an average cross section of $1.8 \times 10^{-14} \text{ cm}^2$ is used. This gives

$$\gamma_{1se}(60^\circ\text{C}) = 220 \text{ s}^{-1}.$$

On the other hand, assuming a cylindrical cell, the last two terms on the right-hand side of equation (7.1.57) are given by equation (3.5.6). For a cell having a length L equal to its diameter D , with $D = 2 \text{ cm}$ as a typical value, one obtains

$$\gamma_{lw} + \gamma_{1BG} = 15.7 D_0 \frac{P_0}{P} + N_0 v_r \sigma_1 \frac{P}{P_0}. \quad (7.1.61)$$

†1 Torr = 133.32 Pa .

Table 7.1.1 Values of the vapour pressure and density of Rb as a function of temperature (1 Torr = 133.32 Pa).

T (K)	P (Torr)	n (cm ⁻³)
280	4.708×10^{-8}	1.624×10^9
285	8.546×10^{-8}	2.895×10^9
290	1.520×10^{-7}	5.060×10^9
295	2.650×10^{-7}	8.674×10^9
300	4.536×10^{-7}	1.460×10^{10}
305	7.629×10^{-7}	2.415×10^{10}
310	1.262×10^{-6}	3.930×10^{10}
315	2.054×10^{-6}	6.295×10^{10}
320	3.292×10^{-6}	9.935×10^{10}
325	5.202×10^{-6}	1.545×10^{11}
330	8.106×10^{-6}	2.372×10^{11}
335	1.246×10^{-5}	3.593×10^{11}
340	1.893×10^{-5}	5.375×10^{11}
345	2.839×10^{-5}	7.946×10^{11}
350	4.210×10^{-5}	1.161×10^{12}

In practice a mixture of argon and nitrogen may be used in order to obtain a low first-order temperature coefficient. If a pressure ratio of 1.5 is used with a total pressure of 25 Torr (3333 Pa), then $P(N_2) = 10$ Torr (1333 Pa) and $P(Ar) = 15$ Torr (2000 Pa). The residual temperature coefficient as calculated from the data of table 3.3.6 is $1.0 \times 10^{-10} \text{ }^\circ\text{C}^{-1}$. This positive temperature coefficient is desirable to compensate for a residual negative temperature coefficient originating from the filter cell and having the same order of magnitude. Using the values of D_0 and σ_1 given in table 3.5.1, one obtains finally

$$\gamma_1 = 306 \text{ s}^{-1}$$

at $60 \text{ }^\circ\text{C}$. In figure 7.1.7 a value of $\gamma_1 = 300 \text{ s}^{-1}$ has been used for illustration.

(b) *Transverse relaxation.* This rate, denoted γ'_2 , is given by equation (7.1.31). It is a decorrelation rate affecting the off-diagonal elements of the density matrix. It contains contributions from the pumping rates and from the coherence relaxation rate γ_2 produced as in the previous case by spin-exchange, wall and buffer gas collisions:

$$\gamma_2 = \gamma_{2se} + \gamma_{2w} + \gamma_{2BG}. \quad (7.1.62)$$

The spin-exchange rate is given by equation (3.6.99). It is equal to

$$\gamma_{2se} = \frac{5}{8}\gamma_{lse} = 138 \text{ s}^{-1}. \quad (7.1.63)$$

Theory

The terms γ_{2w} and γ_{2BG} are given by equation (3.5.9). The first term of this expression, corresponding to diffusion to the wall, i.e. γ_{2w} , is the same as in the calculation of γ_1 . The term γ_{2BG} contains the cross section σ_2 which is not known for ^{87}Rb . It can be calculated, however, with the help of equations (3.3.137) and (3.3.138) using the values of σ_2 for ^{85}Rb given in table 3.5.2. One notes that the part of the cross section originating from the adiabatic process is proportional to the square of the hyperfine structure constant. Using this property, it is found that $\sigma_2(^{87}\text{Rb}) \approx 350 \times 10^{-23} \text{ cm}^2$ for nitrogen. On the other hand, tables 3.5.1 and 3.5.2 show that, for Ar, $\sigma_2(^{85}\text{Rb})$ is smaller than $\sigma_1(^{85}\text{Rb})$. In the case of this buffer gas, the frequency shift is much smaller than in the case of the other gases, and it is not expected that the dispersion in the phase shift due to the modulation of the hyperfine splitting by the collisions will contribute much to the relaxation. In fact it is found that the adiabatic term in equation (3.3.138), which is the second term on the right-hand side, is negligible since $\sigma_2(^{85}\text{Rb}) \approx \frac{3}{4}\sigma_1(^{85}\text{Rb})$. Consequently it is assumed that $\sigma_2(^{87}\text{Rb}) \approx \sigma_2(^{85}\text{Rb}) \approx 37 \times 10^{-23} \text{ cm}^2$ for Ar. A simple calculation then leads to $\gamma_2 = 291 \text{ s}^{-1}$. This is nearly equal to γ_1 and is a typical value found in practice. It leads to population and coherence relaxation times of the order of 3.3 ms.

(c) *The line width.* This is given by

$$\Delta\nu = \frac{1}{\pi} \left(\frac{\Gamma'_2 + \Gamma'_1}{2} + \gamma_2 \right) (S + 1)^{1/2}. \quad (7.1.64)$$

It is a function of position through the pumping rates. It is plotted in figure 7.1.10 as a function of the dimensionless parameter y for the same parameters as those chosen for figure 7.1.7 and $S = 2$. In case B, which is expected to represent the best standard experimental situation, the line width varies from 500 Hz at the entrance of the cell to about 163 Hz at its output. If a cell of optimum length is used, $y_0 \approx 6$ and the average line width is of the order of 375 Hz. This is a typical line width observed in practice.

The line width just calculated assumes that the saturation factor is constant through the cell. This of course is not true in practice since the resonance cell is normally placed in a cavity where b is a function of distance. Furthermore, S is a function of Γ'_1 and Γ'_2 . Consequently S varies with y and the dependence of $\Delta\nu$ on y shown in figure 7.1.10 is an approximation.

The consequence of this behaviour of $\Delta\nu$ versus y has no major effect on the frequency standard performance itself, except through the cavity pulling effect which will be analysed later.

The line width has interesting properties. In fact it can be written in the following manner:

$$W = 2[\gamma'_2^2 + b^2(\text{LEF})]^{1/2} \quad (7.1.65)$$

where (LEF) is the line width enhancement factor introduced by Camparo and Frueholz (1985a,b)

$$\text{LEF} = \gamma'_2 g / (\Gamma'_1 + \gamma_1)(\Gamma'_2 + \gamma_1)(3\Gamma'_1 + 5\Gamma'_2 + 8\gamma_1). \quad (7.1.66)$$

In the absence of optical pumping this factor is simply given by γ_2/γ_1 , which is close to 1 in our case. But in the case where optical pumping is done with a larger rate from one level relative to the other, the LEF can become very large and cause additional line broadening. This broadening is in addition to that caused by the simple consideration of optical pumping as a relaxation process, which is included in γ'_2 . In the case where $\Gamma'_1 = \Gamma'_2 = \Gamma'$ we have LEF = $(\Gamma' + \gamma_2)/(\Gamma' + \gamma_1)$. If γ_2 is nearly equal to γ_1 , this is again close to 1 and the line width is not affected by the phenomenon.

It is worth pointing out that in the previous calculation the effect has been included directly in the definition of S and in equation (7.1.64).

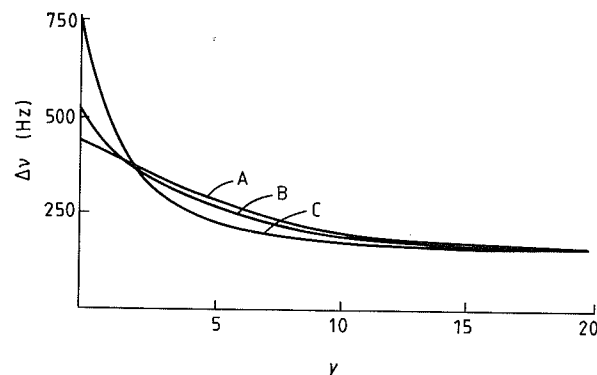


Figure 7.1.10 Variation of the line width with position in the cell for the same conditions as in figure 7.1.7.

(d) *The line shape.* As mentioned earlier, the line shape is approximately Lorentzian. In the case of an optically thin sample we may assume that the Γ'_i do not vary much over the full length of the cell, and the signal as given by equation (7.1.47) may be written

$$\alpha = -\alpha_0 \frac{S}{S+1} \frac{1}{1+x^2/(S+1)} \quad (7.1.67)$$

where α_0 is the maximum fractional signal amplitude observed at $x = 0$ for S large and where x is given by

Theory

$$x = \frac{\omega - \omega_0}{\gamma'_2}. \quad (7.1.68)$$

Equation (7.1.67) is plotted in figure 7.1.11 for various values of S . As will be seen in §7.2, the maximum slope of the discriminator pattern for slow modulation is obtained for $S = 2$, a value which was used in the calculation of the signal amplitude.

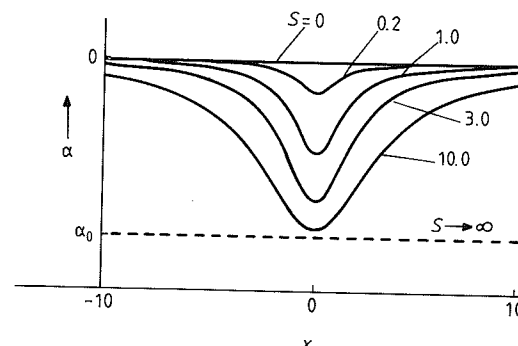


Figure 7.1.11 Plot of the fractional absorption signal for various values of the saturation parameter. The variable x stands for $(\omega - \omega_0)/\gamma'_2$.

(e) *RF power level.* The saturation parameter S is proportional to the square of the magnetic induction at the site of the atoms. In the present case it is given by equation (7.1.29). Using the parameters assumed in the example above, we can calculate the Rabi frequency with $S = 2$:

$$b = 850 \text{ rad s}^{-1}.$$

An average value of $\langle \Gamma'_2 \rangle = 800 \text{ s}^{-1}$ has been assumed, while $\langle \Gamma'_1 \rangle$ has been set equal to zero. In a cavity, the power required to create the above value of the normalised magnetic induction is calculated from the following relation obtained from a previous analysis (see equations (6.1.8) and (6.3.19)):

$$P = \frac{\hbar^2 \omega_0 V_c}{2\mu_0 \mu_B^2 \eta Q_c} b^2. \quad (7.1.69)$$

Assuming a filling factor of about unity, a cavity with a volume of 15 cm^3 and a Q_c of 200, we obtain $P \approx 120 \text{ nW}$.

On the other hand, the power emitted by stimulated emission by the ensemble of atoms exposed to that field is calculated in the following manner. The Rabi frequency may be considered to be the rate at which

transitions are excited between the two states. The emitted power is then approximately the product of the number of atoms by this rate and by the energy quantum $h\nu$. A factor $\frac{1}{2}$ is introduced to take into account the symmetry of the two-level system when transitions take place:

$$P(\text{emitted}) = \frac{h\nu}{2} \frac{b}{2\pi} nV_c. \quad (7.1.70)$$

This gives a power of the order of 1.4×10^{-9} W which is noticeably smaller than the power involved in the previous calculation. Consequently we shall neglect the effect of stimulated emission in all calculations related to passive rubidium frequency standards, except in §7.3.3 when the cavity pulling effect will be considered.

(F) The two-level approximation

It is interesting to compare the results obtained in the present chapter with those obtained in §4.2.5 in the case of a two-level system. The final results are very similar, as shown by equations (4.2.184) and (7.1.47). The main difference comes from the amplitude of the resonance signal. In the two-level system the microwave radiation directly affects the population of the two levels involved, while in the rubidium case only two of the eight levels are affected by the microwave radiation. This difference is taken care of by the constant k in front of the resonant term of the transmitted light expression and by the different definition of the relaxation rates γ'_1 and γ'_2 . Thus in many calculations it is sufficient to use the two-level model if care is taken to define the constants properly in the final equation.

A typical calculation is that involved with the response of the ensemble to a phase- or frequency-modulated microwave signal. This is best done by means of Bloch equations. However, in the case of an eight-level system the problem is very complicated and no analytical solutions exist. Consequently, in view of the similarities of the results obtained in the case of the quasi-static solution for both the two-level and the eight-level systems, the dynamical behaviour of this last system will be analysed as if it were a two-level system. This will be done in Appendix 7A.

In many instances it is sufficient to use the homogeneous approximation. In such a case equation (7.1.47) can be written

$$\mathcal{I}_t = \mathcal{I}_b - \mathcal{I}_0 \left(\frac{S}{S+1} \frac{1}{1 + 4(\omega - \omega_0)^2/W^2} \right) \quad (7.1.71)$$

where \mathcal{I}_b is the background photon flux and $\mathcal{I}_0[S/(S+1)]$ is the resonance signal amplitude. The term \mathcal{I}_0 contains factors which take into account the fact that a multilevel system is analysed. W is the line width given by

$$W = 2\gamma_2 (1 + S)^{1/2} = 2(1 + S)^{1/2}/T_2. \quad (7.1.72)$$

The relaxation rate γ_2 is taken in its general meaning, in which all relaxation rates contributing to a loss of coherence are taken into account.

7.2 DETERMINATION OF THE TRANSITION FREQUENCY

7.2.1 Introduction

As stated in §5.4, the precise location of the frequency of any resonant feature requires information which is proportional to the difference between the interrogation angular frequency ω_i and the transition angular frequency ω_0 [†]. It is provided by the modulation of the frequency or phase of the interrogation signal and by synchronous detection of the response of the resonator under test.

In rubidium gas cell frequency standards the microwave field is often sine wave frequency modulated. The modulation frequency is roughly 30% or more of the line width. It follows that the dynamical behaviour of the atomic medium has to be taken into consideration for an accurate description of its response to the modulation. However, the related analysis is not easy and in §7.2.2 the assumption of a slow modulation will be made at first in order to provide an estimate of the error signal. Square wave frequency modulation will be considered as well as sine wave modulation. Figure 7.2.1 shows the response of a rubidium cell to such modulations.

A detailed analysis of the response of the atomic system when the period of modulation is not large compared with the relaxation times is given in Appendix 7A. It is based on the model described in §7.1. Results are derived for square wave frequency modulation, sine wave phase modulation and square wave phase modulation. Analytical solutions are given whenever possible. However, they can be obtained only under restrictive assumptions such as weak saturation or fast modulation. Nevertheless, they have been developed firstly to provide good examples of calculation techniques which are useful in similar quantum electronic systems and secondly to provide a check of computer solutions which have been worked out to cover operating conditions of practical interest. The computed results are also given in relatively large ranges of variation of the saturation factor, the modulation depth and the modulation frequency. Optimum conditions of modulation are specified.

[†]For the purpose of the following discussion we shall call ω_0 the resonance angular frequency even though this frequency may be displaced by various perturbations.